

## Cooperation between Subunits Is Essential for High-Affinity Binding of *N*-Acetyl-D-hexosamines to Dimeric Soluble and Dimeric Cellular Forms of Human CD69<sup>†</sup>

Daniel Kavan,<sup>‡,§,⊥</sup> Monika Kubíčková,<sup>||,⊥</sup> Jan Bílý,<sup>‡</sup> Ondřej Vaněk,<sup>‡,§</sup> Kateřina Hofbauerová,<sup>§</sup> Hynek Mrázek,<sup>‡,§</sup> Daniel Rozbeský,<sup>‡,§</sup> Pavla Bojarová,<sup>‡,§</sup> Vladimír Křen,<sup>§</sup> Lukáš Židek,<sup>||</sup> Vladimír Sklenář,<sup>||</sup> and Karel Bezouška<sup>\*‡,§</sup>

<sup>‡</sup>Department of Biochemistry, Faculty of Science, Charles University, 12840 Prague, Czech Republic, <sup>§</sup>Institute of Microbiology v.v.i., Academy of Sciences of Czech Republic, 14220 Prague, Czech Republic, and <sup>||</sup>National Centre for Biomolecular Research, Faculty of Science, Masaryk University, 61137 Brno, Czech Republic <sup>⊥</sup>These authors contributed equally to the experiments

Received July 21, 2009; Revised Manuscript Received April 6, 2010

**ABSTRACT:** CD69 is an earliest lymphocyte activation antigen and a universal leukocyte triggering molecule expressed at sites of active immune response. The binding of GlcNAc to the dimeric human CD69 was followed by equilibrium dialysis, fluorescence titration, and NMR. Clear cooperation was observed in the high-affinity binding ( $K_d = 4.0 \times 10^{-7}$  M) of the carbohydrate to two subunits of the dimeric CD69 (Hill coefficient 1.94). A control monosaccharide ManNAc was not bound by human CD69, and both monosaccharides had no effects on the structure of the receptor. However, a monomeric CD69 obtained by mutating Q93 and R134 at the dimer interface exhibited a much lower affinity for GlcNAc ( $K_d = 1.3 \times 10^{-5}$  M) and no cooperativity (Hill coefficient 1.07). Perturbation of the dimer interface resulted in a severe impairment of the signaling ability of cellular CD69 when cross-linked with an antibody or with a bivalent high-affinity *N*-acetylhexosamine dimer-based ligand. The availability of stable preparations of soluble CD69 receptor with well-documented ligand binding properties will be beneficial for immunological experiments evaluating the role of this antigen in the complex environment of the immune system. Moreover, such preparations in combination with efficient ligand mimetics able to both activate CD69<sup>+</sup> lymphocytes and to block undesired hyperactivation caused by other cellular ligands will also become indispensable tools in explaining the exact role of the CD69 antigen in the interaction between the tumor cell and the effector natural killer lymphocyte.

CD69 is an early lymphocyte activation marker and a universal leukocyte triggering molecule expressed at sites of active immune response and chronic inflammation (1, 2). Initial *in vitro* studies suggested that CD69 may function as an activating molecule in many leukocyte subsets including  $\gamma/\delta$  T-cells and natural killer (NK)<sup>1</sup> cells (3, 4). The *CD69* gene is located within the NK gene complex on human chromosome 12. It codes a type II calcium-dependent membrane lectin, a member of one important family of abundant NK cell surface receptors (5, 6) participating in the formation of the receptor “zipper” at the NK cell–tumor cell interface (7). Most receptors of NK cells that recognize target structures at the surface of tumor or virally infected cells mediate their activation or inhibitory effects through their sequentially diverse cytoplasmic domains (8). However, the cytoplasmic domain of CD69 is short and lacks the prominent function-associated peptide motifs. Previous studies have shown that the downstream activation processes initiated by CD69 engagement

occur through Src-dependent activation of Syk, activation of phospholipase C $\gamma$ 2 and Vav, and the subsequent transmission of signals through the Rac–ERK pathway (9, 10). Alternatively, CD69 can also propagate activation signals through heterotrimeric G proteins and the subsequent intracellular signaling pathways coupled to these molecular switches (11, 12). Recently, *in vivo* studies in CD69-deficient mice have added yet another dimension into the biology of this receptor revealing its non-redundant role in downregulation of the immune response through the production of the pleiotropic cytokine TGF- $\beta$  and through interactions with regulatory T-cells (2). Using the same experimental model, it has been shown recently that CD69 forms a complex with sphingosine 1-phosphate receptor, negatively regulates its function, and thus inhibits lymphocyte egress from lymphoid organs downstream of interferon- $\alpha/\beta$ , known mediators of transient egress shut down (13). Furthermore, results of many immunological studies indicate that CD69 may be involved in pathogenesis of several diseases including rheumatoid arthritis, chronic inflammatory liver diseases, mild asthma, and acquired immunodeficiency syndrome (14).

The identification of the natural ligand for CD69 is a key critical step for further advancement of our knowledge on the biology of this receptor. The initial findings that CD69 binds to calcium and certain *N*-acetyl-D-hexosamines (15) could not be later reproduced using a somewhat different expression construct (16). Since then, these discrepancies have been at least partially explained by careful structural evaluations of the recombinant proteins used for binding studies, as well as by

<sup>†</sup>Supported by grants from Ministry of Education of Czech Republic (MSM 21620808, 1M0505, and AVOZ50200510 to K.B. and MSM0021622413 and LC0603 to V.S.) and from Czech Science Foundation (303/09/0477 and 305/09/H008 to K.B. and 203/09/P024 to P.B.) and by EU Project Spine 2 (Contract LSHG-CT-2006-02/220 to K.B.).

\*To whom correspondence should be addressed at Charles University. Phone: +420-2-2195-1272. Fax: +420-2-2195-1283. E-mail: bezouska@biomed.cas.cz.

<sup>1</sup>Abbreviations: DSS, disuccinimidyl suberate; Gal, D-galactose; GlcNAc, *N*-acetyl-D-glucosamine; ManNAc, *N*-acetyl-D-mannosamine; MES buffer, 10 mM MES with 150 mM NaCl and 1 mM Na<sub>2</sub>S<sub>2</sub>O<sub>3</sub>; MES + C buffer, 10 mM MES, 150 mM NaCl, 1 mM CaCl<sub>2</sub>, and 1 mM Na<sub>2</sub>S<sub>2</sub>O<sub>3</sub>; NK, natural killer.

establishing a direct link between the binding of calcium and carbohydrates (17). The proper folding of CD69 produced based on the recently suggested constructs encompassing G70–K199 of the entire receptor was established using detailed structural experiments based on both NMR (18) and protein crystallography (19). The most recent development of efficient structural mimetics of the high-affinity ligand for CD69 opened the way for manipulating with numerous activities of CD69 at the molecular and cellular level (20, 21) and provided efficient compounds for further *in vivo* testing of their immunomodulating properties (22–24).

Here we report new findings indicating that the binding of *N*-acetyl-D-hexosamines to soluble CD69 is highly cooperative at molecular level, and this cooperativity is not seen for Q93A and R134A mutants with disturbed formation of noncovalent dimers. Similarly at the cellular level, efficient signaling after CD69 cross-linking by antibody or bivalent ligand is diminished for the above mutants with a damaged subunit cross-talk more dramatically than for CD69 bearing C68A mutation, and thus lacking the disulfide bridge forming the covalent dimer identified previously as the critical signaling element.

## EXPERIMENTAL PROCEDURES

**Materials.** All chemicals were analytical grade reagents of the best quality available commercially and were obtained from Sigma unless indicated otherwise. The preparation of dimeric *N*-acetylhexosamine disaccharide with the chemical composition (GalNAc $\beta$ 1–4GlcNAc $\beta$ -NH-CS-NH-CH<sub>2</sub>)<sub>2</sub> by a combination of chemical and enzymatic steps has been described previously (25).

**Preparation of Soluble Dimeric CD69.** Preparation of soluble dimeric CD69 using protocol II has been described previously (18). For the preparation of a uniformly <sup>15</sup>N-labeled form of the receptor, a producing culture of *Escherichia coli* BL-21 Gold (Stratagene) harboring the expression plasmid was used, grown on a standard M9 minimal medium containing <sup>15</sup>NH<sub>4</sub>Cl.

**Identification of Key Amino Acid Residues Disrupting the Receptor Dimer Interface.** We examined the three-dimensional structure of the crystallized soluble dimeric CD69 deposited into the RCSB Protein Databank under accession code 3CCK (18). Glutamine Q93 appeared to be involved in two key hydrogen bonds between the amide group of its side chain and two adjacent acidic residues belonging to the opposite subunit, Asp88 and Glu87. With R134, the intertwining with the second subunit is even more profound, and the guanidyl group of this amino acid forms three hydrogen bonds with A136 and Y135 of the opposing subunit and is also involved in the stacking interaction with the phenyl ring of Y135.

**Site-Directed Mutagenesis and Expression of the Mutated CD69 Proteins.** Mutated forms of CD69 in which the Q93 and/or R135 were mutated into A were produced using the CD69 expression plasmid in pRSETB (18). Mutations were introduced using the QuickChange site-directed mutagenesis kit (Stratagene) in combination with the following oligonucleotide pairs: CD69Q93F, 5'-GAGGACTGGGTTGGCTACGCGAG-GAAATGCTACTTTATT-3', and CD69Q93R, 5'-AATAAAGTAGCATTTCCTCGCGTAGCCAACCCAGTCCTC-3', and CD69R134F, 5'-GACATGAACCTTTCTAAAAGCATACGC-AGGTAGAGAGGAA-3' and CD69R134R, 5'-TTCCTCTCT-ACCTGCGTATGCTTTTAGAAAGTTCATGTC. The introduced mutations were verified by DNA sequencing using an

ABI Prism 3130 genetic analyzer (Applied Biosystems). The CD69Q93A/R134A double mutant was prepared sequentially, applying the R134A mutation process on the Q93A mutant. Mutated CD69 proteins were prepared using the same protocol (protocol II) used for the production of the wild-type protein (18). Moreover, the proper refolding of the protein was verified using NMR measurement with the homogeneously <sup>15</sup>N-labeled proteins as described previously (18).

**Gel Filtration.** Gel filtration was performed using a Superdex 200 HR 10/30 column (GE Healthcare) connected to the protein purification system BioSys510 (Beckman Coulter) and equilibrated with MES buffer at room temperature. In order to examine the effect of monosaccharide binding to CD69 on the hydrodynamic volume of the CD69 protein, the protein samples were incubated overnight at 4 °C in the presence of 1 mM ManNAc or 1 mM GlcNAc and then injected onto the gel filtration column equilibrated in MES + C buffer containing 1 mM concentrations of the respective monosaccharides.

**Analytical Ultracentrifugation.** Sedimentation velocity and sedimentation equilibrium experiments were performed using a ProteomeLab XL-I analytical ultracentrifuge (Beckman Coulter) equipped with an An50Ti rotor and dual absorbance and laser interference optics. Before the experiment, 0.5 mL samples of CD69 proteins diluted to 0.4 mg·mL<sup>-1</sup> were dialyzed for 20 h against 2 L of MES + C buffer, with or without the monosaccharides, in concentration indicated in the text, and the dialysis buffer was used as a reference and sample dilution buffer. The sedimentation velocity experiment was conducted at 48000 rpm for dimeric CD69 at 20 °C. Data were analyzed with the program SEDFIT (26, 27). Based on buffer composition and amino acid sequence using the program SEDNTERP (www.jphilo.mailway.com), buffer density and CD69 partial specific volume for CD69NG70 were estimated as 1.00309 g·mL<sup>-1</sup> and 0.7183 mL·g<sup>-1</sup>, respectively.

**Protein Stability Experiments.** CD69 proteins were diluted to 0.5 mg/mL, and UV spectra were taken in the 200–300 nm range in a Beckman DU-70 spectrophotometer (Beckman Coulter) equipped with a heated cuvette. The initial UV scan was taken at 25 °C, after which the temperature in the cuvette was increased in 5 °C increments. Experiments were performed routinely in MES + C buffer. Alternatively, protein stability was verified using differential scanning calorimetry and FTIR spectroscopy as has been previously described (17, 18, 28).

**NMR Titrations.** All NMR experiments were run at 300 K in a Bruker Avance 600 MHz spectrometer equipped with a cryogenic H/C/N TCI probehead. <sup>1</sup>H–<sup>15</sup>N HSQC spectra of 0.3 mM <sup>15</sup>N-labeled wild-type CD69 protein CD69NG70 (18) were used as a routine check of protein folding and stability. The sample buffer consisted of 10 mM MES, pH 5.8, with 49 mM NaCl, 1 mM NaN<sub>3</sub>, and 10% D<sub>2</sub>O. During NMR titration, a 0.1 mM solution of the unlabeled wild-type CD69 protein (7) was titrated. In an initial experiment, aliquots of the GlcNAc ligand corresponding to 25%, 50%, 75%, 100%, 200%, and 500% of saturation were added, and signals of the free GlcNAc ligand were observed at 2.2 ppm in the 1D proton spectra and used for the estimation of the free ligand concentration. In a separate experiment aimed at estimating the binding constant, smaller ligand additions were used as the equivalence was approached. The protein was titrated to 75% of the estimated number of binding sites, after which the amount of ligand was increased in increments of 5% of the estimated number of binding sites until the equivalence point was reached. All spectra were processed

using the software NMRPIPE (29). The dissociation constant  $K_d$ , defined as  $K_d = (c_p - c_L + [L])[L]/(c_L - [L])$ , was obtained by a nonlinear fitting of the  $[L]$  vs  $c_L$  titration curves (Figure 2A,B).

**Equilibrium Dialysis.** *N*-Acetyl-D-[1-<sup>3</sup>H]glucosamine (specific activity 500 GBq/mmol) and *N*-acetyl-D-[1-<sup>3</sup>H]mannosamine (specific activity 650 GBq/mmol) were prepared as described previously (17) or purchased from Amersham. To set up equilibrium dialysis experiments, a rotating apparatus with glass blocks containing separate sealable chambers with external access was used as described previously (17). Aliquots (200  $\mu$ L) of 0.1  $\mu$ M solutions of CD69 proteins in MES + C buffer were incubated with varying amounts of ligand at 27 °C (300 K) for 48 h. After equilibration, 100  $\mu$ L aliquots were withdrawn from the control and from the protein-containing chambers. The results were calculated and plotted according to Scatchard as described previously (17).

**Tryptophan Fluorescence Quenching.** Tryptophan fluorescence quenching experiments were performed according to the described methodology (30) with minor modifications. In initial experiments, 100 nmol aliquots of CD69 protein were pipetted into multiple wells of a UV Star plate (Greiner, Germany) and mixed with 10-fold serial dilutions of the GlcNAc ligand. Incubation proceeded for 1 h at 27 °C (300 K) in the thermostated chamber of a Safire2 plate reader (Tecan, Austria), after which the fluorescence of tryptophan residues was measured in duplicate wells using the bottom fluorescence measurements and the following settings:  $\lambda_{ex}$  = 275 nm,  $\lambda_{em}$  = 350 nm, excitation and emission slits were set to 5 and 20, respectively, and the fluorescence gain was manually set to 66. After finding the lowest concentration of ligand that still caused the quenching of tryptophan fluorescence, detailed dilutions of the ligand by 10% saturation steps were performed, and the concentration of free and bound ligand was calculated as described previously (17, 30).

**Preparation of the Eukaryotic Expression Constructs, Transfection into Jurkat Cells, and Selection of the Transfectants.** In order to mutate the dimerization cysteine C68 (15) to A, site-directed mutagenesis was performed using the original expression plasmid (15) as described above using oligonucleotide primers CD69C68F, 5'-TCAGTGGGCCAATACAATGCTC-CAGGCCAATACACATTC-3', and CD69C68R, 5'-GAATGTGTATTGGCCTGGAGCATTGTATTGGCCCACTGA-3', and the pCDA401 plasmid (15). Single mutation CD69C68A, double mutations CD69C68A/Q93A and CD69C68A/R134A, and the triple mutation CD69C68A/Q93A/R134A were prepared by applying the mutagenesis protocol onto expression plasmids for wild-type CD69 (8) and for the respective dimerization mutants described above. After the mutagenesis and DNA sequencing, DNA fragments coding the C-terminal extracellular segments of CD69 were linked with the DNA fragment coding the N-terminal part of the receptor (31) using linking PCR (8). The X construct corresponded to the religated pCR3 (mock) and was used as a control (8). The eukaryotic expression vectors were sequenced and transfected into a Jurkat T lymphoblastoid cell line maintained in RPMI1640 and supplemented with 10% fetal calf serum (8).

**Precipitation of Cellular Forms of CD69 Using Antibodies and Dimeric *N*-Acetylhexosamines.** Transfected Jurkat cells ( $1 \times 10^6$ ) were surface radioiodinated using lactoperoxidase (31), washed three times with medium, and then incubated with 1 mM concentrations of dimeric *N*-acetylhexosamine disaccharides for 1 h at room temperature. The incubation was followed by the addition of 100 mM DSS and by cross-linking

of the receptors for another 1 h at 4 °C. Thereafter, cells were lysed, and CD69 receptor complexes were immunoprecipitated using G protein beads (GE Healthcare) coated with monoclonal antibodies against CD69, BL-KFB/B1 (31). Beads were washed extensively, boiled in sample buffer for SDS-PAGE, and analyzed using 15% SDS-polyacrylamide gels followed by autoradiography.

**Cellular Activation Assays and Production of IL-2.** Transfected Jurkat cells ( $10^6$ ) were incubated with dimeric *N*-acetylhexosamine disaccharides as described in the preceding section or with saturating concentrations of monoclonal antibodies against CD69 for 5 min (cellular activation) or 12 h (IL-2 production) and used to determine the free cytoplasmic calcium (11) or IL-2 production (8).

## RESULTS AND DISCUSSION

**Evaluation of Calcium and Carbohydrate Binding Activity of Highly Stable CD69 Proteins.** We and others have previously generated several constructs optimized for the preparation of highly stable soluble recombinant CD69 proteins suitable for ligand identification experiments (Supporting Information Table S1). Preliminary ligand binding experiments were performed to evaluate the ability of these constructs to bind calcium and monosaccharides shown to be important ligands for the receptor (15, 17). With regard to the binding of calcium, there has been no difference in the ability to bind calcium between the covalent dimeric protein CD69CQ65 and noncovalent dimeric proteins CD69NG70 and CD69NV82 when compared to the monomeric protein CD69MS100: each of these proteins bound 1 mol of calcium/mol of CD69 subunit with  $K_d$  of approximately 58  $\mu$ M (ref 17 and Supporting Information Figure S1). On the other hand, significant differences between these protein constructs were observed with regard to the binding of *N*-acetyl-D-hexosamines. While the  $IC_{50}$  values for the soluble monomeric CD69, CD69MS100, with regard to binding of the two active *N*-acetyl-D-hexosamines, D-GlcNAc and D-GalNAc, were each approximately  $10^{-5}$  M, these values were about 10 times lower for the dimeric protein CD69NV82 and about 100 times lower for the other two highly stable dimeric proteins, CD69CQ65 and CD69NG70 (Supporting Information Figure S2). The latter protein has been selected for all of the subsequent binding experiments and will be referred to as soluble dimeric CD69. The homogeneity and monodispersity were routinely evaluated for each batch of the produced soluble dimeric CD69 using SDS electrophoresis under both reducing and nonreducing conditions and gel filtration on a Superdex 200 HR column (ref 18 and Figure 1). Moreover, the identity, quality, and proper refolding of each batch of the produced protein were also verified as described previously (18) using high-resolution ion cyclotron resonance mass spectrometry, one-dimensional proton NMR, thermal stability experiments, and tests of the biochemical stability (ref 18 and Table 1).

**Cooperativity of GlcNAc Binding Proved by Direct Binding Experiments.** The detailed binding studies with soluble dimeric CD69 were performed using D-GlcNAc as the high-affinity carbohydrate ligand, together with D-ManNAc and, in some experiments, D-Gal as negative controls. The initial evidence for the interaction of the soluble dimeric CD69 with GlcNAc was obtained by NMR titration. A 0.1 mM solution of the dimeric receptor was titrated up to equivalence assuming the existence of two high-affinity binding sites per receptor



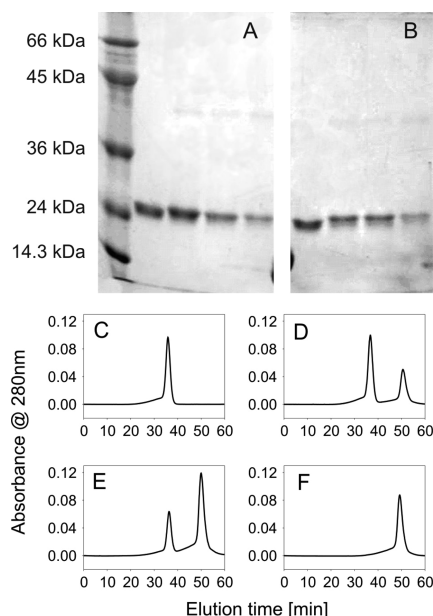


FIGURE 1: Analysis of wild-type and mutant CD69 proteins by SDS–PAGE and gel filtration. In (A) and (B), these proteins were analyzed under reducing and nonreducing conditions, respectively. Analyzed proteins, from left to right, were wild-type CD69, CD69Q93A mutant, CD69R134A mutant, and CD69QRDM. Marker proteins were BSA (65 kDa), ovalbumin (44 kDa), lactoglobulin (18 kDa), lysozyme (14 kDa), and aprotinin (6 kDa). In (C) to (F), these proteins were analyzed by gel filtration on a Superdex 200 HR column, and the four respective panels contain chromatograms for wild-type CD69, CD69Q93A mutant, CD69R134A mutant, and CD69QRDM double mutant.

Table 1: Summary of Stability Properties of Wild-Type Dimeric CD69 and CD69 Dimerization Mutants

protein	characteristics	$T_d^a$ (°C)	$T_d^b$ (°C)	$T_d^c$ (°C)
CD6CD69WT	noncovalent dimers	65	67	65
CD69Q93A	dimer/monomer equilibrium	63	62	64
CD69R134A	dimer/monomer equilibrium	62	60	60
CD69QRDM	monomeric	60	62	61

<sup>a</sup>Determined from thermal UV denaturation measurements. <sup>b</sup>Determined from differential scanning calorimetry. <sup>c</sup>Determined from FTIR spectroscopy.

dimer (17). The results of this experiment (Figure 2B and Supporting Information Figure S3B) confirmed the specific binding of GlcNAc to the receptor (2 mol of GlcNAc bound to a receptor dimer) and provided an affinity estimation in the low micromolar range ( $K_d = 4.0 \times 10^{-7}$  M). On the other hand, no interaction could be seen with the ManNAc negative control under the same experimental conditions (Figure 2A and Supporting Information Figure S3A). However, NMR did not enable the fraction of the bound ligand to be measured.

In order to confirm the results obtained by NMR titration, additional direct binding experiments were performed. When the bound and the unbound ligands had been separated by dialysis under equilibrium, two binding sites per receptor dimer were detected. Direct binding experiments enabled the degree of saturation at each particular ligand concentration to be calculated. The resulting saturation curve, showing the saturation (fraction bound normalized per receptor subunit) dependence on the ligand concentration (Figure 2C), clearly revealed a striking cooperativity in the highly specific ( $K_d = 4.0 \times 10^{-7}$  M) binding

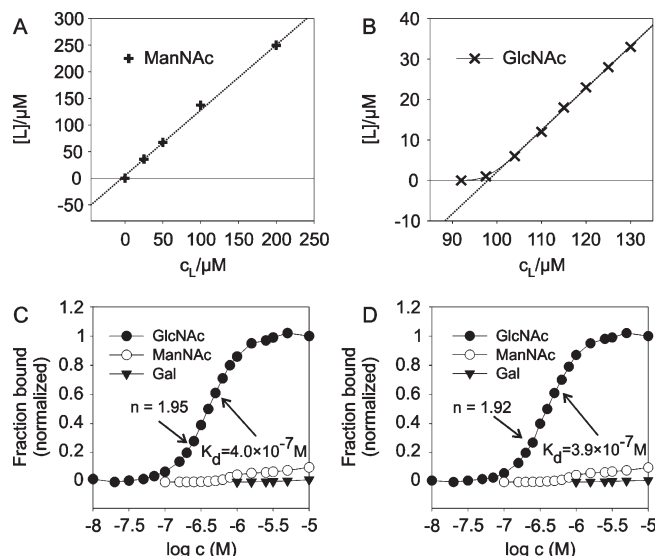


FIGURE 2: Measurements of direct interaction of soluble CD69NG70 with ManNAc and GlcNAc. (A, B) NMR titration of soluble CD69 with ManNAc and GlcNAc, respectively. (C, D) Concentration dependence of receptor saturation measured by equilibrium dialysis and tryptophan fluorescence quenching, respectively, using GlcNAc, ManNAc, and Gal as indicated.

of GlcNAc to the receptor with the Hill coefficient approaching the maximum theoretical value (theory 2.00, experiment 1.95; see Figure 2C). These results were also independently confirmed by the third binding assay, the fluorescent titration, which gave binding parameters essentially identical to those obtained by the equilibrium dialysis (Figure 2D). On the other hand, very little specific binding for both ManNAc and Gal control monosaccharides could be seen in both of the latter assays (Figure 2C,D).

**Binding of N-Acetyl-D-hexosamines Did Not Result in Significant Conformational Change in CD69 Protein.** To analyze the structural changes of soluble CD69 upon ligand binding, variations in the hydrodynamic properties of the receptor were investigated. The molecular size of the receptor, which had been saturated with an excess of GlcNAc, was studied by gel filtration on Superdex 200 HR and by analytical ultracentrifugation and compared with the size of the receptor preincubated in the ManNAc control. The elution time decrease from 36.5 to 31.7 min in the gel filtration would indicate a change in the molecular size of CD69 upon GlcNAc binding when compared to the presence of ManNAc (Supporting Information Figure S4). However, the detailed analysis of soluble dimeric CD69 in the absence of any ligand, in the presence of 1 mM ManNAc, and in the presence of 1 mM GlcNAc did not reveal any changes in hydrodynamic properties since the value of the experimentally determined sedimentation coefficient was identical (Supporting Information Figure S5).

**Binding of N-Acetyl-D-glucosamine to the Stable Monomeric CD69 Follows a Single Site Model and Proceeds with Much Lower Affinity.** In the next step, the interactions of GlcNAc with the monomeric subunit of CD69 were studied. Since it proved extremely difficult to prepare the monomeric form of the receptor by dissociation of the CD69 dimer (18), we used the available crystal structure of the CD69 dimer and analyzed the dimer interface for critical residues participating in the dimerization. Two such critical residues, namely Q93 and R134, both interacting with two residues of the other subunit, could be identified (Supporting Information Figure S6).

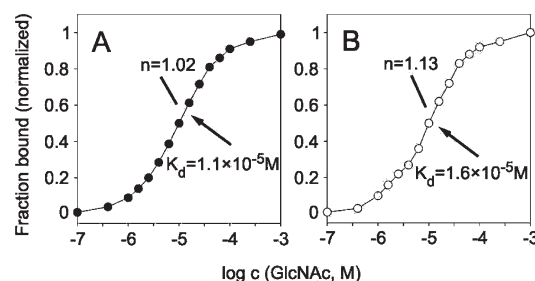


FIGURE 3: Binding of GlcNAc to the monomeric subunit of CD69. (A, B) Binding of GlcNAc to monomeric CD69 analyzed using equilibrium dialysis and fluorescence titration, respectively.

These amino acid residues were mutated to alanine, singly or in combination. All three produced mutated proteins were after their refolding and purification extensively verified using the methodology described previously (18) for the wild-type protein CD69NG70 using SDS electrophoresis and ion cyclotron resonance mass spectrometry of the entire protein, as well as nuclear magnetic resonance to check the proper folding of these proteins (Figure 1 and results not shown). The stability of the mutant soluble CD69 proteins was comparable to that of the wild-type protein, indicating that the introduced mutations did not result in any decrease of protein stability. Only the double mutant behaved as a monomeric protein (Figure 1), with stability comparable to that of the dimer receptor (Table 1). This protein was used to analyze the binding of GlcNAc to the monomeric subunit of CD69. The results clearly showed that binding to the monomeric subunit of CD69 was much weaker and noncooperative (Hill coefficient of 1.07; Figure 3).

**Q93/R134/C68 Triple Mutation Is Necessary to Disrupt the Dimerization of the Cellular Form of CD69.** The soluble CD69 receptor used in the first part of this study utilized a previously described construct CD69NG70 (18) that refolded as a noncovalent soluble dimer from a polypeptide consisting of amino acids G70–K199 (Supporting Information Table S1). This construct contained an extended dimer interface involved in contacts between the ligand binding domains, as well as the neck regions. However, it did not contain the C68 residue that has been shown (8, 15) to participate in the covalent dimerization of the natural form of CD69 found at the surface of leukocytes. It thus appeared interesting to look into the effects of mutations of the critical residues C68, Q93, and R134 at the CD69 dimer interface on the structure and on the well-documented signaling functions of the cellular form of CD69. In order to trigger the CD69-mediated activation of transfected Jurkat cells bearing both wild-type and mutated forms of CD69, an efficient ligand is required for receptor cross-linking. Alternatively, the receptor can be aggregated using specific antibodies. In the experiments presented here, we used both forms of activation using two specific cross-linking monoclonal antibodies against CD69, BL-KFB/B1 and BL-Ac/p26, as well as the *N*-acetylhexosamine disaccharide dimer (Figure 4B), which has been previously described (25) as the most efficient carbohydrate ligand at enabling precipitation (and thus cross-linking) of the soluble CD69. The structurally closely related ligand, *N*-acetylglucosamine dimer (Figure 4A), served as a suitable negative control in these experiments.

We transferred inserts coding the CD69 receptors into a eukaryotic expression vector for the transfection of the Jurkat T-lymphocyte leukemic cell line (refs 9 and 10 and Table 2). Those clones displaying identical surface expression of the wild-type and mutated receptors (as shown by flow cytometry) were

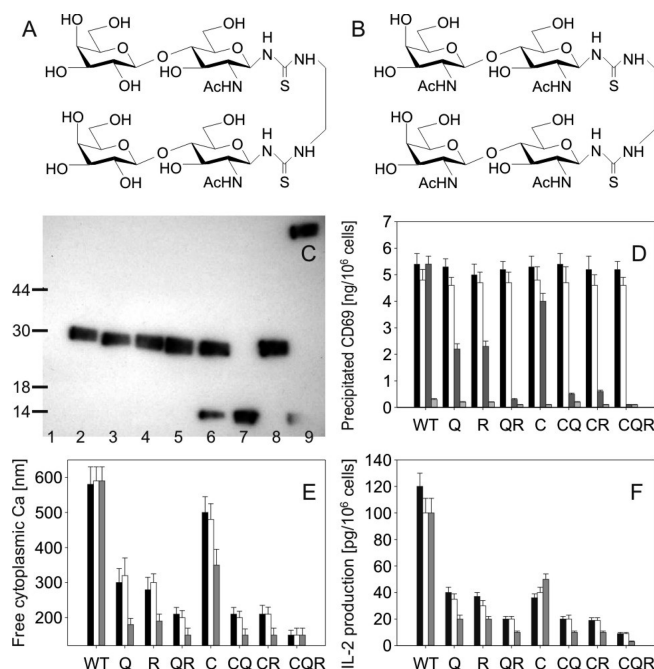


FIGURE 4: Analysis of cellular CD69 on transfected cells and evaluation of binding and signaling efficiency of receptor disturbed at the dimer interface. (A, B) Chemical formulas of *N*-acetylglucosamine and *N*-acetylhexosamine disaccharide dimer, respectively. (C) Surface expression of CD69 immunoprecipitated from control non-transfected cells (lane 1) or from cells containing wild-type CD69 (lane 2), CD69Q93A (lane 3), CD69R134A (lane 4), CD69C68A/Q93A (lane 5), C68A/R134A (lane 6), C68A/Q93A/R134A (lane 7), C68A/Q93A/R134A cross-linked with *N*-acetylhexosamine disaccharide dimer (8) (lane 8), and wild-type CD69 cross-linked with *N*-acetylhexosamine disaccharide dimer (lane 9). Receptors were surface-labeled using lactoperoxidase, dimerized using DSS cross-linking, immunoprecipitated, and analyzed by SDS electrophoresis under reducing conditions followed by autoradiography. (D) Precipitation of various forms of wild-type and mutated CD69 using *N*-acetylglucosamine or *N*-acetylhexosamine disaccharide dimer and antibodies against CD69. (E) Cellular activation of Jurkat leukemic T-cells transfected with wild-type or mutated CD69 with mutations at the dimer interface. (F) Production of IL-2 by Jurkat leukemic T-cells transfected with wild-type or mutated CD69 with mutations at the dimer interface. The designation of mutants in (D) to (F) is based on the mutated amino acids and their combinations: C, C68; Q, Q93; R, R134. The cellular CD69 in (D) to (F) was cross-linked using monoclonal antibody BL-KFB/B1 (2) (left columns), monoclonal antibody BL-Ac/p26 (2) (middle columns), or *N*-acetylhexosamine disaccharide dimer (right columns). The fourth, small column in (D) placed after the three above-mentioned columns indicates precipitation with *N*-acetylglucosamine control.

subcloned, frozen, and used in individual experiments (Figure 5). First, the molecular forms of the surface CD69 were analyzed in both native and ligand cross-linked receptors. In order to determine the precise molecular forms of the receptors in these experiments, native receptors were fixed by di(*N*-hydroxysuccinimido) suberate (DSS), shown previously to produce covalent dimers with soluble CD69 (I. Polakovičová, unpublished observation), before their extraction from the plasma membrane and molecular analysis. Cellular CD69 bearing single mutations in amino acids responsible for the covalent (C68) or noncovalent (Q93, R134) dimerization remained mostly dimeric, as did the double mutants C68A/Q93A, C68A/R134A (Figure 4C, lanes 2–6), and Q93/R134 (not shown). Only the triple mutant C68A/Q93A/R134A was completely monomeric (Figure 4C, lane 7). However, this monomeric protein could still be efficiently dimerized by the *N*-acetylhexosamine disaccharide dimer (lane 8), which caused

Table 2: Characterization of Individual Clones of Jurkat T-Cell Leukemia Transfected with CD69 Isoforms<sup>a</sup>

CD69 isoform	clone	general characteristic	CD69 expression by FACS <sup>b</sup>	used for expts
CD69WT	WT1	good growth	10	no
	WT2	<b>moderate growth</b>	<b>30</b>	<b>yes</b>
	WT3	moderate growth	80	no
CD69Q93A	Q1	good growth	20	no
	Q2	<b>good growth</b>	<b>30</b>	<b>yes</b>
	Q3	moderate growth	70	no
CD69R134A	R1	moderate growth	30	yes
	R2	<b>good growth</b>	<b>90</b>	<b>no</b>
CD69QRDM	RQ1	moderate growth	10	no
	RQ2	<b>good growth</b>	<b>30</b>	<b>yes</b>
	RQ3	good growth	70	no
CD69C68A	C1	<b>good growth</b>	<b>30</b>	<b>yes</b>
	C2	good growth	60	no
CD69CQDM	CQ1	good growth	10	no
	CQ2	<b>moderate growth</b>	<b>30</b>	<b>yes</b>
	CQ3	moderate growth	80	no
CD69CRDM	CR1	moderate growth	10	no
	CR2	<b>moderate growth</b>	<b>30</b>	<b>yes</b>
	CR3	slow growth	90	no
CD69CQRTM	CQR1	moderate growth	10	no
	CQR2	good growth	20	no
	CQR3	<b>moderate growth</b>	<b>30</b>	<b>yes</b>
	CQR4	slow growth	60	no

<sup>a</sup>Only the successful transformants with relative fluorescence intensity of CD69 expression between 10 and 100 have been included into this table.

<sup>b</sup>Median of relative fluorescence intensity from FACS analyses at the top of the peak.

extensive cross-linking and formation of high molecular weight aggregates in wild-type cellular CD69 (lane 9).

*Mutations in Q93 and R134 of Cellular CD69 Result in More Significant Impairment in Its Signaling than Mutation in C68.* We further investigated the effect of mutations destabilizing the dimerization of cellular CD69 on the cross-linking of this receptor and its function in cellular activation. While all of the expressed cellular CD69 could be efficiently cross-linked by two monoclonal antibodies against this antigen, the cross-linking by the dimerized ligand was severely impaired in the mutants affecting receptor dimerization even if the dimerization process *per se* was not affected (cf. Figure 4C,D). Interestingly, mutations in the amino acids forming the noncovalent dimer interface had in several instances a more profound effect than the mutation in C68 responsible for covalent dimerization. On the other hand, no precipitation of the receptor occurred when the *N*-acetyllactosamine dimer control compound was used (Figure 4D).

Subsequently, the influence of the mutations affecting the dimerization of cellular CD69 on the ability of this receptor to activate the Jurkat cell line, as documented by the increase in the intracellular calcium levels, was analyzed. Strikingly, even if the cellular CD69 antigens bearing the above mutations could be fully cross-linked by binding to monoclonal antibodies, their ability to confer activation was severely affected (Figure 4E). For instance, single mutations in amino acids at the noncovalent dimer interface (i.e., Q93A or R134A mutations) lowered the efficiency of these receptors in cellular signaling by two-thirds. On the other hand, when using ligand cross-linking with the *N*-acetylhexosamine disaccharide dimer, a very low efficiency of cellular signaling was observed compared to the wild-type

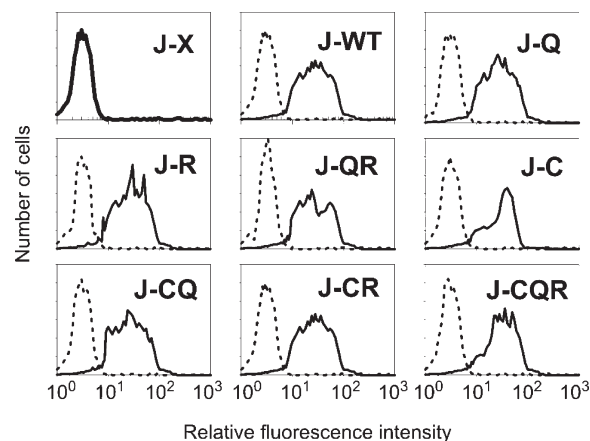


FIGURE 5: Analysis of surface expression of cellular CD69 in transfected Jurkat cell clones as determined by flow cytometry: J-X, insert-free (mock DNA) transfectant; J-WT, cells transfected with wild-type CD69; J-Q, cells transfected with CD69Q93A mutant; J-R, cells transfected with CD69R134A mutant; J-QR, cells transfected with CD69Q93A/R134A double mutant; J-C, cells transfected with CD69C68A mutant; J-CQ, cells transfected with CD69C68A/Q93A double mutant; J-CR, cells transfected with CD69C68A/R134A double mutant; J-CQR, cells transfected with CD69C68A/Q93A/R134A triple mutant. Reactivity with the monoclonal antibody against CD69 (BL-KFB/B1) is shown by the solid line; reactivity with the isotype-matched control antibody against NKR-P1 (HD14) is shown by the dotted line.

controls (Figure 4E). This may be explained by a combination of low efficiency of ligand binding and receptor cross-linking together with a direct effect on signaling efficiency. Similar results were obtained with the production of IL-2 as another measure of cellular activation (Figure 4F).

## CONCLUSIONS

The results presented here indicate that the binding of carbohydrate ligands to both the soluble and cellular forms of CD69 is cooperative and is affected by the interaction of the two subunits of this receptor. This is a hitherto unreported observation, since the signaling through CD69 has been so far ascribed exclusively to its association with the signaling adapter proteins in the transmembrane region of the molecule (8). Thus, while the previous studies have defined the role of the individual polypeptide segments of CD69 in cellular expression, surface dimerization, and cellular signaling, the present results are unique in emphasizing the role of the intact dimer interface in the receptor molecule that was found to be much larger than the mere cysteine 68 thought previously (8, 15) to be critical for receptor dimerization. Moreover, our findings suggest a novel mechanism for sensitive ligand recognition by CD69 and related immune receptors. Within the C-type lectin family, various alternative strategies have been employed to attain high-affinity binding. Classical hepatic lectins are oligomeric proteins in which the individual carbohydrate-recognition domains within the oligomer cooperate during the recognition of desialylated glycoproteins (32). Other members of this protein family employ alternative calcium-dependent processes to achieve this goal (33). Among the receptors of the immune system, the soluble mannose-binding protein again employs a multiple carbohydrate-recognition domain to bind specifically to surface polysaccharides of various pathogens and activate their effector functions such as opsonization or complement activation (34, 35). Compared to these lectins, lymphocyte receptors forming group V of



the C-type lectin family are much smaller and mostly dimeric, and thus they seem to have developed alternative strategies for their recognition of specific ligands. These are based either on oligomerization of the receptor within the specialized plasma membrane microdomains of the immune cell (36) or on alternative strategies that may be used by some of these receptors (37). The molecular mechanism that we propose based on the results of the current work is unique in rapid propagation of the activation signal using the mechanism of rapid cooperative receptor cross-linking and oligomerization based on the positive cooperativity in binding of the multivalent ligands.

## ACKNOWLEDGMENT

We thank Angela Risso for assistance and helpful discussions, Iva Polakovičková for help with DSS cross-linking experiments, and Michal Navrátil for help in the development of cellular receptor precipitation assays.

## SUPPORTING INFORMATION AVAILABLE

A description of additional experimental procedures with supporting references, binding of calcium to the fourth generation soluble CD69 proteins (Figure S1), carbohydrate inhibition experiments for these proteins (Figure S2), primary data for NMR titrations with ManNAc and GlcNAc (Figure S3), elution profiles for gel filtration of soluble dimeric CD69 (CD69NG70) in the absence of ligand as well as in the presence of 1 mM ManNAc and 1 mM GlcNAc (Figure S4), sedimentation velocity experiments with CD69NG70 in the absence of ligand and in the presence of 1 mM ManNAc and 1 mM GlcNAc (Figure S5), identification of amino acids for the design of the monomeric CD69 mutant (Figure S6), and characterization of CD69 expression constructs (Table S1). This material is available free of charge via the Internet at <http://pubs.acs.org>.

## REFERENCES

- Testi, R., D'Ambrosio, D., De Maria, R., and Santoni, A. (1994) The CD69 receptor: a multipurpose cell surface trigger for hematopoietic cells. *Immunol. Today* 15, 479–483.
- Sancho, D., Gómez, M., and Sánchez-Madrid, F. (2005) CD69 is an immunoregulatory molecule induced following activation. *Trends Immunol.* 26, 136–140.
- Moretta, A., Poggi, A., Pende, D., Tripodi, G., Orenco, A. M., Pella, N., Augugliaro, R., Bortino, C., Ciccone, E., and Moretta, L. (1991) CD69-mediated pathway of lymphocyte activation: anti-CD69 monoclonal antibodies trigger the cytolytic activity of different lymphoid effector cells with the exception of cytolytic T lymphocytes expressing T cell receptor  $\alpha/\beta$ . *J. Exp. Med.* 174, 1393–1398.
- Borrego, F., Robertson, M. J., Ritz, J., Pena, J., and Solana, R. (1999) CD69 is a stimulatory receptor for natural killer cells and its cytotoxic effect is blocked by CD94 inhibitory receptor. *Immunology* 97, 159–165.
- Lopez-Cabrera, M., Santis, A. G., Fernandez-Ruiz, F., Blacher, R., Esch, F., Sanchez-Mateos, P., and Sánchez-Madrid, F. (1993) Molecular cloning, expression, and chromosomal localization of the human early activation antigen AIM/CD69, a new member of C-type lectin superfamily of signal-transmitting receptors. *J. Exp. Med.* 178, 537–547.
- Lanier, L. L. (2008) Up on the tightrope: natural killer cell activation and inhibition. *Nat. Immunol.* 9, 495–502.
- Vivier, E., Tomasello, E., Baratin, M., Walzer, T., and Ugolini, S. (2008) Functions of natural killer cells. *Nat. Immunol.* 9, 503–510.
- Sancho, D., Santis, A. G., Alonso-Lebrero, J. L., Viedma, F., Tejedor, R., and Sánchez-Madrid, F. (2000) Functional analysis of ligand-binding and signal transduction domains of CD69 and CD23 C-type lectin leukocyte receptors. *J. Immunol.* 165, 3868–3875.
- Pisegna, S., Zingoni, A., Pirozzi, G., Cinque, B., Cifoni, M. G., Morrone, S., Piccoli, M., Frati, L., Palmieri, G., and Santoni, A. (2002) Src-dependent Syk activation controls CD69 mediated signaling and function of human NK cells. *J. Immunol.* 169, 68–74.
- Zingoni, A., Palmieri, G., Morrone, S., Carretero, M., Lopez-Botet, M., Piccoli, M., Frati, L., and Santoni, A. (2000) CD69-triggered ERK activation and functions are negatively regulated by CD94/NKG2A inhibitory receptors. *Eur. J. Immunol.* 30, 644–651.
- Risso, A., Smilowich, D., Capra, M. C., Baldissarro, I., Yan, G., Bargiessi, A., and Cosulich, M. E. (1991) CD69 in resting and activated T lymphocytes. Its association with a GTP binding protein and biochemical requirements for its expression. *J. Immunol.* 146, 4105–4114.
- Bikah, G., Pogue-Caley, R. R., and McHeyzer-Williams, M. G. (2000) Regulating T helper cell immunity through antigen responsiveness and calcium entry. *Nat. Immunol.* 1, 402–412.
- Shiow, R. L., Rosen, D. B., Brdečková, N., Xu, Y., An, J., Langer, L. L., Cyster, J. G., and Matloubian, M. (2006) CD69 acts downstream of interferon- $\alpha/\beta$  to inhibit S1P<sub>1</sub> and lymphocyte egress from lymphoid organs. *Nature* 440, 540–544.
- Marzio, R., Mauel, J., and Betz-Corradin, S. (1999) CD69 and regulation of the immune functions. *Immunopharmacol. Immunotoxicol.* 21, 565–582.
- Bezouška, K., Nepovím, A., Horváth, O., Pospíšil, M., Hamann, J., and Feizi, T. (1995) CD69 antigen of human leukocyte is a calcium-dependent carbohydrate-binding protein. *Biochem. Biophys. Res. Commun.* 208, 68–74.
- Childs, R. A., Galustian, C., Lawson, A. M., Doufán, G., Benwell, K., Frankel, G., and Feizi, T. (2000) Recombinant soluble human CD69 dimer produced in *Escherichia coli*: reevaluation of saccharide binding. *Biochem. Biophys. Res. Commun.* 266, 19–23.
- Pavlíček, J., Sopko, B., Ettrich, R., Kopecký, V., Baumruk, V., Man, P., Havlíček, V., Vrbáček, M., Martinková, L., Křen, V., Pospíšil, M., and Bezouška, K. (2003) Molecular characterization of binding of calcium and carbohydrates by an early activation antigen of lymphocytes CD69. *Biochemistry* 42, 9295–9306.
- Vaněk, O., Nálezková, M., Kavan, D., Borovičková, I., Pompach, P., Novák, P., Kumar, V., Vannucci, L., Hudeček, J., Hofbauerová, K., Kopecký, V., Brynda, J., Kolenko, P., Dohnálek, J., Kadeřávek, P., Chmelík, J., Gorčík, L., Židek, L., Sklenář, V., and Bezouška, K. (2008) Soluble recombinant CD69 receptors optimized to have an exceptional physical and chemical stability display prolonged circulation and remain intact in the blood of mice. *FEBS J.* 275, 5589–5606.
- Kolenko, P., Skálová, T., Vaněk, O., Štěpánková, A., Dušková, J., Hašek, J., Bezouška, K., and Dohnálek, J. (2009) The high-resolution structure of the extracellular domain of human CD69 using a novel polymer. *Acta Crystallogr. F65*, 1258–1260.
- Pavlíček, J., Kavan, D., Pompach, P., Novák, P., Lukšan, O., and Bezouška, K. (2004) Lymphocyte activation receptors: new structural paradigm in group V of C-type animal lectins. *Biochem. Soc. Trans.* 32, 1124–1126.
- Bezouška, K., Šnajdrová, R., Křenek, K., Vančurová, M., Kádek, A., Adámek, D., Lhoták, P., Kavan, D., Hofbauerová, K., Man, P., Bojarová, P., and Křen, V. (2010) Carboxylated calixarenes bind strongly to CD69 and protect CD69<sup>+</sup> killer cells from suicidal cell death induced by tumor cell surface ligands. *Bioorg. Med. Chem.* 18, 1434–1440.
- Křenek, K., Kuldová, M., Hulíková, K., Stibor, I., Lhoták, P., Dudič, M., Budka, J., Pelantová, H., Bezouška, K., Fišerová, A., and Křen, V. (2007) N-acetyl-D-glucosamine substituted calix[4]arenes as stimulators of NK cell-mediated antitumor immune response. *Carbohydr. Res.* 342, 1781–1792.
- Hulíková, K., Benson, V., Svoboda, J., Šima, P., and Fišerová, A. (2009) N-Acetyl-D-glucosamine-coated polyamidoamine dendrimer modulates antibody formation via natural killer cell activation. *Int. Immunopharmacol.* 9, 792–799.
- Benson, V., Grobárová, V., Richter, J., and Fišerová, A. (2010) Glycosylation regulates NK cell-mediated effector function through PI3K pathway. *Int. Immunol.* 22, 167–177.
- Bojarová, P., Křenek, K., Wetjen, K., Adamiak, K., Pelantová, H., Bezouška, K., Elling, L., and Křen, V. (2009) Synthesis of LacdiNAc-terminated glycoconjugates by mutant galactosyltransferase—A way to new glycodrugs and materials. *Glycobiology* 19, 509–517.
- Schuck, P. (2000) Size distribution analysis of macromolecules by sedimentation velocity ultracentrifugation and Lamm equation modelling. *Biophys. J.* 78, 1606–1619.
- Schuck, P. (2003) On the analysis of protein self-association by sedimentation velocity analytical ultracentrifugation. *Anal. Biochem.* 320, 104–124.
- Dousseau, F., Therrien, M., and Pézole, M. (1989) On the spectral subtraction of water from the FT-IR spectra of aqueous solution of proteins. *Appl. Spectrosc.* 43, 538–542.

29. Delaglio, F., Grzesiek, S., Vuister, G. W., Zhu, G., Pfeifer, J., and Bax, A. (1995) NMRPipe: a multidimensional spectral processing system based on an UNIX pipes. *J. Biomol. NMR* 6, 277–293.
30. Chipman, D. M., Grisaro, V., and Sharon, N. (1967) The binding of oligosaccharides containing *N*-acetylglucosamine and *N*-acetylmuramic acid to lysozyme. *J. Biol. Chem.* 242, 4388–4394.
31. Hamann, J., Fiebig, H., and Strauss, M. (1993) Expression cloning of the early activation antigen CD69, a type II integral membrane protein with a C-type lectin domain. *J. Immunol.* 150, 4920–4927.
32. Blomhoff, R., Tolleshaug, H., and Berg, T. (1982) Binding of calcium ions to the isolated asialoglycoprotein receptor. Implication for receptor function in suspended hepatocytes. *J. Biol. Chem.* 257, 7456–7459.
33. Kimura, T., Imai, Y., and Irimura, T. (1995) Calcium-dependent conformation of a mouse macrophage calcium-type lectin. Carbohydrate binding activity is stabilized by an antibody specific for a calcium-dependent epitope. *J. Biol. Chem.* 270, 16056–16062.
34. Weis, W. I., and Drickamer, K. (1994) Trimeric structure of a C-type mannose-binding protein. *Structure* 15, 1227–1240.
35. Wallis, R., and Drickamer, K. (1999) Molecular determinant of oligomer formation and complement fixation in mannose-binding proteins. *J. Biol. Chem.* 274, 3580–3589.
36. Diefenbach, A., and Raulet, D. H. (2001) Strategies for target cell recognition by natural killer cells. *Immunol. Rev.* 181, 170–184.
37. Coombs, P. J., Harrison, R., Pemberton, S., Quintero-Martinez, A., Parry, S., Haslam, S. M., Dell, A., Taylor, M. E., and Drickamer, K. (2010) Identification of novel contributions to high-affinity glycoprotein-receptor interactions using engineered ligands. *J. Mol. Biol.* 396, 685–696.